J Mater Sci (2009) 44:5263–5273
DOI 10.1007/s10853-009-3559-8

FERROELECTRICS

Electrothermal properties of perovskite ferroelectric films

J. Zhang · A. A. Heitmann · S. P. Alpay · G. A. Rossetti Jr.

Received: 6 May 2009 / Accepted: 9 May 2009 / Published online: 10 June 2009

Abstract The electrothermal properties of the perovskite oxides barium titanate (BTO), lead titanate (PTO), and strontium titanate (STO) are computed near the temperatures of their ferroelectric and/or ferroelastic phase transitions. The computations are performed using a modified 2-4-6 Ginzburg–Landau–Devonshire polynomial as functions of applied electric field and temperature for mechanically free monodomain crystals and for epitaxial thin films subject to perfect lateral clamping. For BTO and PTO, which display weak first-order ferroelectric phase transitions at their Curie points, the application of a bias field exceeding the electrical critical point reduces the dependence of the electrocaloric (EC) response on temperature and automatically reduces its magnitude. Under conditions of perfect lateral clamping, the weak first-order phase change is transformed into second-order phase change. In this instance the electrical critical point is coincident with the Curie temperature and a lower bias field is required to produce a comparable reduction in temperature sensitivity. Comparison of the electrothermal behaviors of BTO and PTO with that computed for STO near the temperature of the second-order ferroelastic phase transition provides insight concerning the EC properties of ferroelectric solid solution systems wherein the Curie temperature and the first-order character of the paraelectric to ferroelectric transition both may change subject to a change in composition. The results illustrate how electrical and mechanical boundary conditions can be adjusted, in conjunction with composition, in altering the EC properties of ferroelectric materials selected for use in a particular temperature range.

J. Zhang · A. A. Heitmann · S. P. Alpay · G. A. Rossetti Jr. (✉)
Materials Science and Engineering Program and Institute of Materials Science, University of Connecticut, Storrs, CT 06269, USA
e-mail: rossetti@ims.uconn.edu

Introduction

Electrocaloric (EC) materials have recently attracted considerable interest for use in solid-state cooling devices. Such devices may find applications, for example, in thin film micro-coolers used as thermal management systems for next generation integrated circuits or other high power density microelectronic components. The EC effect is a coupling between the electrical and thermal properties of a dielectric solid wherein an adiabatic change in temperature (ΔT) is produced in response to a change in applied electric field. The EC effect and the converse effect of pyroelectricity are described by the same property coefficient, $p = (\partial S/\partial E)_T = (\partial P/\partial T)_E$, where S is entropy, T is temperature, E is electric field, and P is the electric polarization. The property coefficient p is non-zero only for crystals belonging to one of the 10 polar point groups, in which there exists a unique polar axis. Ferroelectric crystals represent a sub-group of these, wherein the spontaneous polarization may be reoriented among symmetry equivalent directions under the application of an electric field.

Ferroelectric materials based on the perovskite-structured oxides have long been considered as prime candidates for use in EC devices and their electrothermal properties have been studied since the 1960s [1–3]. These early studies, carried out primarily on bulk polycrystalline specimens, indicated that the EC properties that could be achieved are comparatively small ($\Delta T < 2$ K) and restricted to a very narrow temperature interval adjacent to the ferroelectric Curie point, where the spontaneous electric

polarization exhibits its maximum rate of change with temperature. However, it was recently reported by Mischenko et al. [4] that much larger EC responses could be realized at modest voltages (~25 V) in the ferroelectric solid solutions $PbZrO_3$–$PbTiO_3$ (PZT) and $Pb(Mg_{1/3}Nb_{2/3})O_3$–$PbTiO_3$ (PMN–PT) [5] when these were prepared as thin film materials with thicknesses of ~300 nm. By driving these thin films above a high electric bias field (~300 kV/cm), large EC effects were evident over a broad temperature range with peak adiabatic temperature changes reaching as much as $\Delta T \sim 12$ K. These findings immediately stimulated a resurgence of interest in the EC properties of ferroelectric materials. Since this time, the literature on both experimental and theoretical aspects of the topic has been steadily growing [6–15]. Moreover, it has very recently been reported that large EC effects are observed in some ferroelectric copolymer systems, such as poly(vinylidene fluoride–trifluoroethylene) [P(VDF–TrFE)] [16], inviting new possibilities for the development of composite or other hybrid materials systems.

In previous work [6, 7], we reported a thermodynamic analysis of the EC properties of $BaTiO_3$ (BTO) under both mechanically free (bulk) and laterally clamped (thin film) conditions. It was shown that the large EC effects as observed experimentally in PZT and PMN–PT films are of the same order of magnitude as the intrinsic stress-free monodomain response in BTO provided that the electric bias field is large enough to completely suppress the characteristic discontinuities in thermodynamic properties at the weak first-order paraelectric (PE) to ferroelectric (FE) phase change. It was further shown that as with the dielectric and piezoelectric properties, the alteration of the PE–FE phase transition that can arise as a consequence of the electromechanical coupling between the spontaneous electric polarization and the internal stress field in thin film structures also has a pronounced influence on the EC response. In particular, perfect lateral clamping transforms the weak first-order PE–FE transition in BTO into a second-order transition, decreasing both the magnitude of the EC effect and the dependence of the effect on temperature. Naturally, misfit strains also alter the nature of the ferroelectric phase transition and thus produce changes in the EC response as well. Indeed it was shown that for a given choice of electrical bias field, a compressive misfit strain shifts the maximum in the EC response to higher temperature, reduces its magnitude, and decreases its dependence on temperature as compared to the laterally clamped film. Tensile misfit strains produce just the opposite results.

These findings highlight the importance of appropriately choosing electrical and mechanical boundary conditions in experimental studies of electrothermal coupling phenomena in thin film ferroelectric materials. At the same time, the nature of the PE–FE phase transition in the mechanically free (bulk) crystal is another significant factor that must also be taken into consideration. To illustrate this point, we have computed the EC properties of $PbTiO_3$ (PTO) and we compare them here to those of BTO. Although both ferroelectric materials display weak first-order transitions at their respective Curie points, as judged by the difference between their Curie and Curie–Weiss temperatures, the first-order character of the PE–FE phase change in PTO is appreciably stronger as compared to BTO. Here we investigate this difference in phase transition characteristics in connection with its effect on the resulting EC properties. In addition, we make a formal extension of the thermodynamic analysis as applied to the ferroelectric perovskites BTO and PTO to the 'incipient' ferroelectric $SrTiO_3$ (STO). Computations are performed for these materials as functions of applied electric field and temperature under both mechanically free and clamped boundary conditions. The results demonstrate how experimental conditions must be adjusted in order to obtain valid comparisons of the EC performance characteristics of ferroelectric materials having different phase change behaviors. The results also carry implications concerning the EC properties of ferroelectric solid solution systems comprising the end member compounds BTO, PTO, and STO, wherein both the Curie temperature and nature of the PE–FE transition may be expected to change subject to a variation in composition.

Thermodynamic theory

The starting point for the analysis of the EC properties of ferroelectric BTO and PTO is the classical 2-4-6 Ginzburg–Landau–Devonshire polynomial [17, 18] expressed in powers of the polarization vector $\mathbf{P} = \{P_1, P_2, P_3\}$. Assuming isothermal conditions and considering only the PE–FE transition between the cubic ($Pm3m$) and tetragonal ($P4mm$) phases, the expansion of the free energy density for the monodomain single crystal in the unconstrained state reduces to

$$G_{\text{bulk}}(T, E, P) = G_0 + \alpha_1 P^2 + \alpha_{11} P^4 + \alpha_{111} P^6 - EP, \quad (1)$$

where G_0 is the free energy density of the paraelectric phase. In the tetragonal ferroelectric state $P_1 = P_2 = 0$, and $P_3 = P \neq 0$ is the component of the electric polarization directed along one of the cube axes of the high-symmetry phase. Here E is a component of the applied electric field, oriented parallel to the polarization direction, and α_1, α_{11}, and α_{111} are dielectric stiffness coefficients. The quadratic coefficient α_1 is given by the Curie–Weiss Law, $\alpha_1 = \alpha_0(T - T_C)$, where $\alpha_0 = 1/(2\varepsilon_0 C)$, ε_0 is the permittivity of free space, T_C is the Curie temperature, and C is the Curie–Weiss constant. The higher-order dielectric

Table 1 Landau coefficients and thermodynamic properties of BTO and PTO (in SI units, the temperature T in K) [23]

	BTO	PTO
T_C	383	752
α_1	$3.3(T\text{-}383) \times 10^5$	$3.8(T\text{-}752) \times 10^5$
α_{11}	$3.6(T\text{-}448) \times 10^6$	-7.3×10^7
α_{111}	6.6×10^9	2.6×10^8
Q_{12}	-0.043	-0.026
C_{11}	1.76×10^{11}	1.75×10^{11}
C_{12}	8.46×10^{10}	7.94×10^{10}

stiffness coefficients α_{11} and α_{111} are, in principle, also analytical functions of temperature. The Curie temperatures, Landau coefficients, and other thermodynamic parameters used in the computations for BTO and PTO are given in Table 1.

In the unconstrained state, STO does not display a ferroelectric transition, although such a transition can be induced in thin film materials by internally generated (or in bulk crystals by externally imposed) stress fields [19–21]. Under stress-free conditions, a structural phase transformation takes place below the temperature T_{st} to a centrosymmetric tetragonal phase belonging to space group *I4/mcm*. This *ferroelastic* transition involves a rotation of the oxygen octahedra about the cube axes of the high-symmetry cubic (*Pm3m*) phase. The order parameter for the structural phase transformation is given by $\mathbf{q} = \{q_1, q_2, q_3\}$ with $q_1 = q_2 = 0$ and $q_3 = q \neq 0$, and the free energy density for stress-free monodomain crystal can be expressed as:

$$G_{\text{bulk}}(T, E, q, P) = G_0 + \beta_1 q^2 + \beta_{11} q^4 + \alpha_1 P^2 + \alpha_{11} P^4 - t_{11} P^2 q^2 - EP. \quad (2)$$

Here, β_1 and β_{11} are the structural order parameter susceptibility coefficients, t_{11} is the coupling coefficient between the structural order parameter q and the field-induced polarization P, and α_1 and α_{11} are the dielectric stiffness coefficients. The structural transition temperature, the Landau coefficients and other thermodynamic properties used in the computations for STO are collected in Table 2.

When $E = 0$, the spontaneous polarization (P_S) in the tetragonal ferroelectric phases of BTO and PTO follows from the condition of thermodynamic equilibrium:

$$\frac{dG_{\text{bulk}}}{dP} = \alpha_1 + 2\alpha_{11} P^2 + 3\alpha_{111} P^4 = 0, \quad (3)$$

or

$$P_S^2(T) = \frac{-\alpha_{11} + \sqrt{\alpha_{11}^2 - 3\alpha_1 \alpha_{111}}}{3\alpha_{111}}. \quad (4)$$

Table 2 Landau coefficients and thermodynamic properties of STO (in SI units, the temperature T in K) [25]

	STO
T_{st}	105
α_1	$4.05\left[\coth\left(\frac{54}{T}\right) - \coth\left(\frac{54}{30}\right)\right] \times 10^7$
α_{11}	2.03×10^9
C_{11}	3.181×10^{11}
C_{12}	1.025×10^{11}
Q_{11}	1.251×10^{10}
Q_{12}	-1.08×10^9
β_1	$1.32\left[\coth\left(\frac{145}{T}\right) - \coth\left(\frac{145}{105}\right)\right] \times 10^{29}$
β_{11}	1.94×10^{50}
λ_{11}	1.3×10^{30}
λ_{12}	-2.5×10^{30}
t_{11}	-3.366×10^{29}

When $E \neq 0$, the equilibrium polarization P^0 has contributions that arise from both the spontaneous polarization and the induced polarization, and its value is determined from the equation of state,

$$\partial G_{\text{bulk}}/\partial P = E. \quad (5)$$

For STO, the equilibrium condition for $E = 0$ (and thus $P = 0$) is given by,

$$\partial G_{\text{bulk}}/\partial q = 0, \quad (6)$$

or

$$q_S(T) = \pm\sqrt{-\frac{\beta_1}{2\beta_{11}}}. \quad (7)$$

When $E \neq 0$, the condition of thermodynamic equilibrium gives

$$\partial G_{\text{bulk}}/\partial q = 0 \quad (8)$$

$$\partial G_{\text{bulk}}/\partial P = E \quad (9)$$

yielding two expressions that must be solved simultaneously,

$$\beta_1 q + 2\beta_{11} q^3 - t_{11} P^2 q = 0, \quad (10)$$

$$2\alpha_1 P + 4\alpha_{11} P^3 - 2t_{11} P q^2 = E. \quad (11)$$

For thin film materials, the free energy density has to be modified to take into account the internal stresses that may arise from lattice and thermal expansion mismatch between the film and substrate, the self strain of the phase transformation, and the clamping effect of the substrate. Here we consider a particular case of epitaxial BTO, PTO, and STO films deposited on a cubic substrate and wherein the orientation is $(001)_{\text{film}}//(001)_{\text{substrate}}$. Considering the mechanical boundary conditions for this situation, [i.e., equal in-plane biaxial stress components (in contacted notation) $\sigma_1 = \sigma_2$, no shear stresses ($\sigma_4 = \sigma_5 = \sigma_6 = 0$)

and no out-of-plane stress ($\sigma_3 = 0$)], the free energy density for the ferroelectrics BTO and PTO can be expressed as:

$$G_{\text{film}}(T, E, P, u_m) = G_0 + \alpha_1 P^2 + \alpha_{11} P^4 + \alpha_{111} P^6 - EP + G_{\text{el}}. \quad (12)$$

The elastic energy term, G_{el}, is given by:

$$G_{\text{el}} = \tilde{C}\left(u_m - Q_{12}P^2\right)^2. \quad (13)$$

Here, u_m is the in-plane polarization-free misfit strain which is defined as:

$$u_m = \frac{a_{\text{substrate}} - a_{\text{film}}}{a_{\text{substrate}}}, \quad (14)$$

and $Q_{12}P^2$ is the self-strain due to polarization, Q_{ij} are the cubic electrostrictive coefficients in polarization notation, and $\tilde{C}$ is an effective elastic modulus,

$$\tilde{C} = C_{11} + C_{12} - \frac{2C_{12}^2}{C_{11}}, \quad (15)$$

where C_{ij} are the elastic stiffnesses at constant polarization. After some rearrangement we obtain [22],

$$G_{\text{film}}(T, E, P, u_m) = G_0 + \tilde{\alpha}_1 P^2 + \tilde{\alpha}_{11} P^4 + \alpha_{111} P^6 - EP + u_m^2 \tilde{C}, \quad (16)$$

with modified dielectric stiffness coefficients given by:

$$\tilde{\alpha}_1 = \alpha_1 - 2u_m Q_{12} \tilde{C}, \quad (17)$$

$$\tilde{\alpha}_{11} = \alpha_{11} + Q_{12}^2 \tilde{C}. \quad (18)$$

It should be noted if we consider an epitaxial film with no in-plane strain ($u_m = 0$), the Curie temperatures T_C of the ferroelectrics BTO and PTO will not change relative to their values in the unclamped state, since $\tilde{\alpha}_1 = \alpha_1$ in Eq. 17. However, the order of the phase transformation *may be changed* due to the two-dimensional clamping of the film by the substrate as described by $\tilde{\alpha}_{11}$, which is *not* a function of the misfit strain u_m. Hence, if the phase transformation in the unconstrained single crystal is of first-order (i.e., $\alpha_{11} < 0$), the phase transformation in the corresponding epitaxial film may be of second-order, depending on the magnitude of $Q_{12}^2 \tilde{C}$. When the external field $E = 0$, minimization of the modified free energy with respect to the polarization ($dG_{\text{film}}/dP = 0$) yields the spontaneous polarization of the film as a function of the misfit strain,

$$P_S^2(T, u_m) = \frac{-\tilde{\alpha}_{11} + \sqrt{\tilde{\alpha}_{11}^2 - 3\tilde{\alpha}_1 \alpha_{111}}}{3\alpha_{111}}. \quad (19)$$

We limit our discussion here only to the phase transformation from a cubic non-polar to a tetragonal ferroelectric "c-domain" phase. As shown theoretically for BTO and PTO, other tetragonal variants and non-tetragonal ferroelectric phases may also form depending on the sign and magnitude of the misfit strain [23]. These have not been considered in this study but can be included by modifying the Landau potential to take into account all components of the polarization vector and the corresponding elastic/electrostrictive energies associated with the additional polarization components. Furthermore, the theoretical approach may be expanded to include polydomain formation as well [24].

To describe the effects of mechanical boundary conditions on the structural phase transformation in thin film STO, we adopt the particular form of the free energy density given by Pertsev et al. [25],

$$G_{\text{film}}(T, E, q, P, u_m) = G_0 + \tilde{\beta}_1 q^2 + \tilde{\beta}_{11} q^4 + \tilde{\alpha}_1 P^2 + \tilde{\alpha}_{11} P^4 - \tilde{t}_{11} P^2 q^2 - EP, \quad (20)$$

in which the re-normalized (structural and dielectric) stiffness and coupling coefficients are,

$$\tilde{\beta}_1 = \beta_1 + 2\left(\frac{C_{12}}{C_{11}}\lambda_{11} - \lambda_{12}\right)u_m, \quad (21)$$

$$\tilde{\beta}_{11} = \beta_{11} - \frac{\lambda_{11}^2}{2C_{11}}, \quad (22)$$

$$\tilde{\alpha}_1 = \alpha_1 + 2\left(\frac{C_{12}}{C_{11}}Q_{11} - Q_{12}\right)u_m, \quad (23)$$

$$\tilde{\alpha}_{11} = \alpha_{11} - \frac{Q_{11}^2}{2C_{11}}, \quad (24)$$

$$\tilde{t}_{11} = t_{11} + \frac{Q_{11}\lambda_{11}}{C_{11}}. \quad (25)$$

Here, the λ_{ij} are the coupling coefficients between the strain and the structural order parameter in contracted notation, and their values are listed in Table 2. For $E = 0$, the shift in the ferroelastic transformation temperature as a function of u_m is given by Eq. 21 and the two-dimensional clamping effect of the substrate is described by Eq. 22. The equilibrium structural order parameter for $E = 0$ can be determined from Eq. 7 with re-normalized stiffness coefficients $\tilde{\beta}_1$ and $\tilde{\beta}_{11}$. In the presence of an applied electric field E, the condition for thermodynamic equilibrium is given by the equations of state $\partial G_{\text{film}}/\partial q = 0$ and $\partial G_{\text{film}}/\partial P = E$ such that:

$$\begin{aligned} &\tilde{\beta}_1 q + 2\tilde{\beta}_{11} q^3 - \tilde{t}_{11} P^2 q = 0 \\ &2\tilde{\alpha}_1 P + 4\tilde{\alpha}_{11} P^3 - 2\tilde{t}_{11} P q^2 = E \end{aligned} \quad (26)$$

For simplicity, we do not take into account the possibility of the formation of other ferroelastic/ferroelectric phases as discussed theoretically in Ref. [25] as the only phase transformation for $u_m = 0$ is from a non-polar cubic to a non-polar tetragonal phase.

For a constant applied electric field, the excess entropy S^{XS}, the excess specific heat ΔC, and the EC coefficient p for BTO and PTO can be determined through the relations,

$$S_E^{XS}(T,E) = -\left(\frac{\partial G^0}{\partial T}\right)_E, \tag{27}$$

$$\Delta C_E(T,E) = -T\left(\frac{\partial^2 G^0}{\partial T^2}\right)_E, \tag{28}$$

$$p(T,E) = \left(\frac{\partial P^0}{\partial T}\right)_E = \left(\frac{\partial S}{\partial E}\right)_T. \tag{29}$$

Equation 29 can be rearranged to explicitly determine the adiabatic temperature change (ΔT) due to the EC effect in ferroelectric materials arising from a change in the applied electric field. By computing values of C_E and P^0 as functions of T and E, this temperature change can be determined through,

$$\Delta T(T,E) = -T\int_{E_a}^{E_b} \frac{1}{C_E}\left(\frac{\partial P^0}{\partial T}\right)_E dE, \tag{30}$$

where $E_b - E_a = \Delta E$ is the change in electric field strength. In the general case, the adiabatic temperature change ΔT occurring in a FE film in response to an applied electric field is a function of both the temperature and the internal strain. However, under the condition of in-plane clamping ($u_m = 0$), the ΔT computed in response to an applied electric field is only a function of temperature for both bulk and thin film FE materials.

STO has a centrosymmetric (non-polar) crystal structure above and below the structural phase transformation temperature both in bulk and in thin film form when $u_m = 0$. Accordingly, it does not exhibit an EC response, and per the definitions given in Eq. 29 and 30, both p and ΔT are equal to zero (there is no spontaneous polarization). However, as the applied electric field E induces a polarization, an *electrothermal* temperature change can be computed from Eq. 30 which corresponds to a temperature variation that arises from the change in the excess specific heat due to the T and E dependencies of the structural order parameter q.

For all materials considered in this study, the absolute value of specific heat, $C_E(T,E)$, was estimated by scaling the computed zero-field values of the excess specific heat $\Delta C_E(T,E)$ given in Eq. 28 to the lattice or "hard mode" contributions taken from the experimental values [9] measured over temperature intervals away from those where the FE phase transitions or structural transition are located.

Results and discussion

In comparing the EC behaviors of the ferroelectric compounds BTO and PTO, it is first instructive to consider the nature of the ferroelectric transitions that occur at the Curie points in these two materials. Because both materials exhibit weak first-order transitions that are close to second-order, it is useful to define a parameter that characterizes degree of deviation from a second-order phase change. Following the usual approach of the Landau theory, this parameter is easily recognized as the relative difference between the Curie temperature T_C and the temperature T_{PF} where the PE and FE phases are in thermal equilibrium in the stress-free crystal,

$$\Delta = \frac{T_{PF} - T_C}{T_C} = \frac{\alpha_{11}^2}{4\alpha_0\alpha_{111}T_C}. \tag{31}$$

It follows from Eq. 31 that $(T_{PF} - T_C) \to 0$ as the quartic dielectric stiffness coefficient $\alpha_{11} \to 0$, and under this condition, the transition becomes second-order. The point in the general electric field–temperature–stress phase diagram of a ferroelectric crystal where a line of first-order transitions passes over to a line of second-order transitions is known as a tricritical point. This is the point where two lines of electrical critical points having opposite signs of E intersect the line of second-order phase transitions. Using the Landau coefficients listed in Table 1, a measure of the degree of deviation from this point for the stress-free crystal at zero field may be estimated as $\Delta \cong 0.013$ for BTO, while in PTO it is about 50% larger, $\Delta \cong 0.019$.

With these considerations in mind, it is now useful to compare the family of curves $P(T)|_E$ and $C_E(T)|_E$ for BTO and PTO at different field strengths E under both mechanically free and clamped boundary conditions. The computed results for BTO ($\Delta = 0.013$) are shown in Fig. 1. Naturally, the application of the field conjugate E of the order parameter P destroys the discontinuities in thermodynamic properties at the temperature T_{PF} of the first-order PE–FE phase change. As seen in Fig. 1a, for BTO, a field strength 10 kV/cm is sufficiently large to do so. However, the curve P(T) in this field exhibits an inflection point at $T > T_{PF}$ and the second derivative properties, such as the specific heat C_E, will therefore exhibit a well-defined maximum, as shown in Fig. 1b. As the field strength is increased, the inflection point will move to higher temperatures, and the gradient of the curve at this point, $\partial P/\partial T$, will diminish. At still higher field strengths the value of $\partial P/\partial T$ at the infection point will be substantially reduced because the majority contribution to the total polarization is induced by the electric field. For mechanically free BTO, a comparison of Fig. 1a, b indicates that this behavior occurs for field strengths exceeding $E \sim 100$ kV/cm. Under mechanically clamped conditions, the family of curves $P(T)|_E$ and $C_E(T)|_E$ are qualitatively similar, as shown in Fig. 1c and d. However, perfect lateral clamping transforms the zero-field first-order phase transition in to a second-order one, and a much lower field strength $E \sim 50$ kV/cm is required to achieve the same effect as

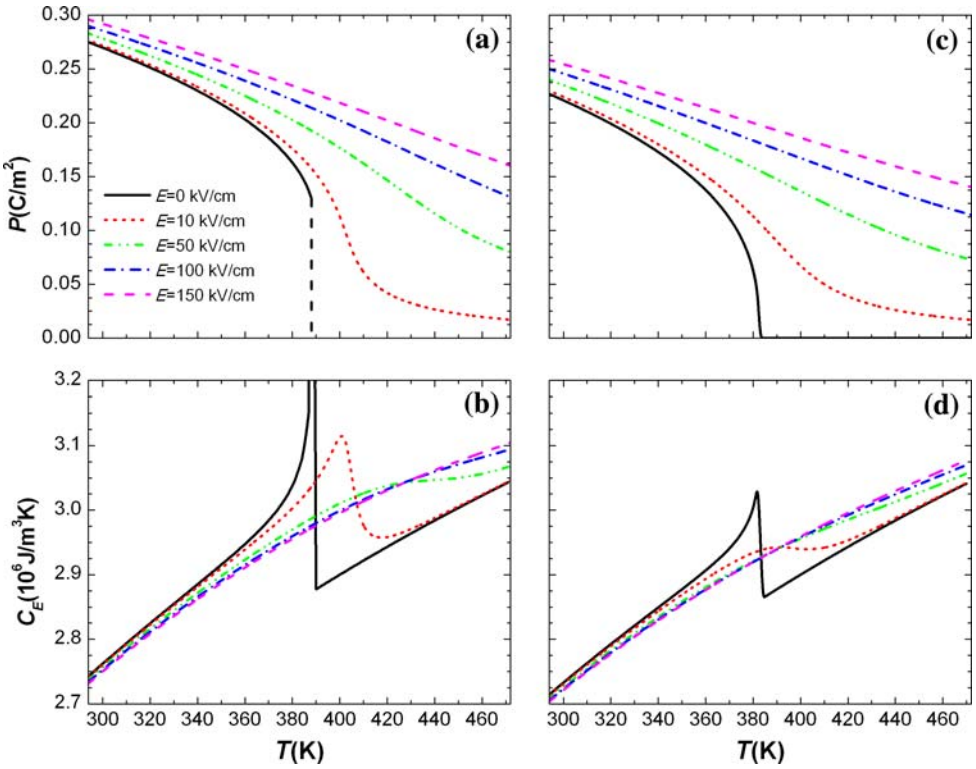

Fig. 1 Plots of polarization and specific heat as functions of temperature and applied electric field for monodomain BTO in the mechanically free state (**a** and **b**), and under prefect lateral clamping (**c** and **d**) (Color online)

observed at 100 kV/cm in the stress-free crystal. As can be appreciated by comparing Eq. 18 with Eq. 31, the zero-field first-order transition ($\alpha_{11} < 0$) is transformed into a second-order one under the condition that the product $Q_{12}^2\tilde{C}$ is sufficiently large.

The corresponding family of curves $P(T)|_E$ and $C_E(T)|_E$ are shown for PTO under mechanically free and clamped boundary conditions in Fig. 2. It is clear that owing to the stronger first-order PE–FE phase change in PTO ($\Delta = 0.019$) the results will differ, but only quantitatively, from those shown for BTO on Fig. 1. In this connection there are, however, several points worthy of note. First, despite the stronger first-order phase change in PTO as compared with BTO, the effect of perfect lateral clamping is the same. The product $Q_{12}^2\tilde{C}$ is again larger than the absolute value of the quartic dielectric stiffness coefficient α_{11}, and the zero-field first-order transition becomes of second-order under mechanical clamping. Second, inspection of Fig. 2a reveals that, in contrast to the weaker first-order phase change in BTO, a field strength $E = 10$ kV/cm is not sufficient to destroy the discontinuities in first derivative thermodynamic properties for the mechanically free crystal. Inspection of Fig. 2a and b shows that at some field $0 < E < 50$ kV/cm there should exist an electrical critical point, where both $\partial P/\partial T$ and C_E approach infinity. Very close to this point, the EC effect will be maximal but also show a strong dependence on temperature over a very narrow range. Finally, it is clear that even at field strengths as large as $E = 150$ kV/cm, remnants of the temperature variation of the spontaneous polarization due to the phase change persist in both the mechanically free and clamped states to temperatures that are significantly higher than the transition temperatures, T_{PF} and T_C, respectively. This is evidenced by the weak maxima observed in the specific heat curves, as shown in Fig. 2c and d.

The effect of an electric field on the ferroelastic phase change in STO is, of course, fundamentally different. In STO all of the polarization is induced by the applied field, and as seen in Fig. 3a and c, the $P(T)|_E$curves change little with changes in temperature and mechanical boundary constraints. In this instance, the main effect of an applied field is to shift the temperature T_{st} of the second-order ferroelastic phase change to lower temperatures, as can be seen by the behavior of the specific heat shown in Fig. 3b and d. Physically interpreted, the effect of the electric field is to oppose the rotation of the oxygen octahedra about the (pseudo-cubic) fourfold axis oriented normal to the film surface, stabilizing the higher symmetry cubic phase relative to the lower temperature tetragonal phase. Under different mechanical boundary conditions (e.g., with $u_m \neq 0$) a non-polar phase could be induced, and this simple picture would be modified.

Recalling that the experimental measurement conditions for the EC effect are defined by the Maxwell relation, $p = (\partial S/\partial E)_T$, the influence of the differing phase transition behaviors described above on the EC responses can best be

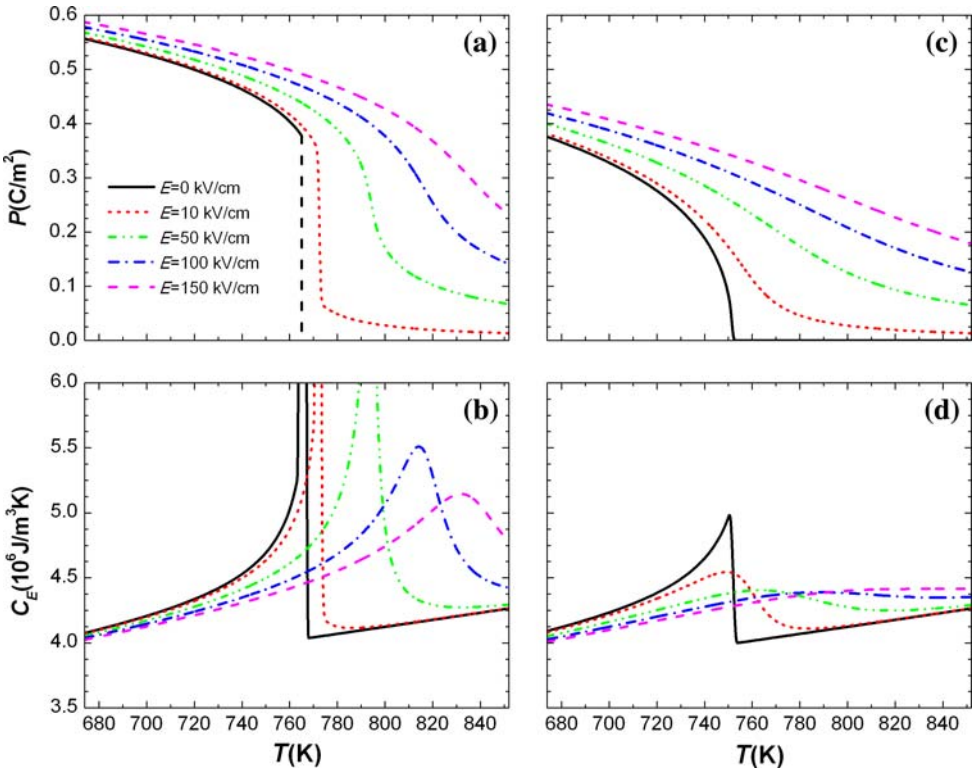

Fig. 2 Plots of polarization and specific heat as functions of temperature and applied electric field for monodomain PTO in the mechanically free state (**a** and **b**), and under prefect lateral clamping (**c** and **d**) (Color online)

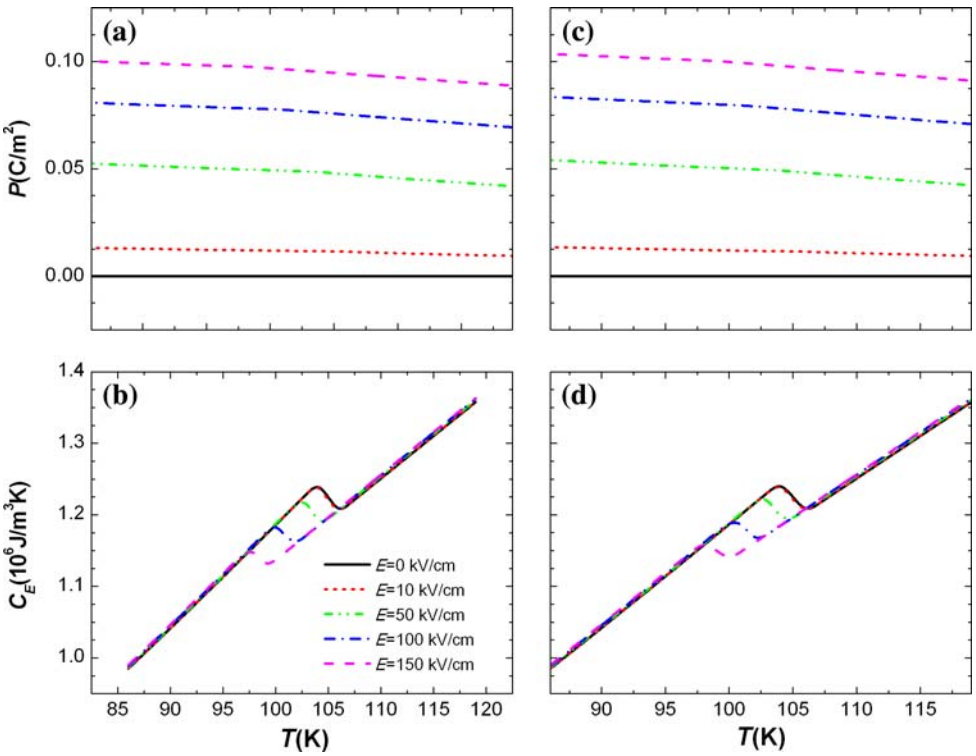

Fig. 3 Plots of polarization and specific heat as functions of temperature and applied electric field for monodomain STO in the mechanically free state (**a** and **b**), and under prefect lateral clamping (**c** and **d**) (Color online)

appreciated by examining the field dependence of the excess entropy along lines of constant temperature. The results computed for BTO under mechanically free and clamped conditions are shown in Fig. 4. For the mechanically free crystal it is seen in Fig. 4a that, on increasing the field from an initial value $E_a = 0$ to a nonzero field

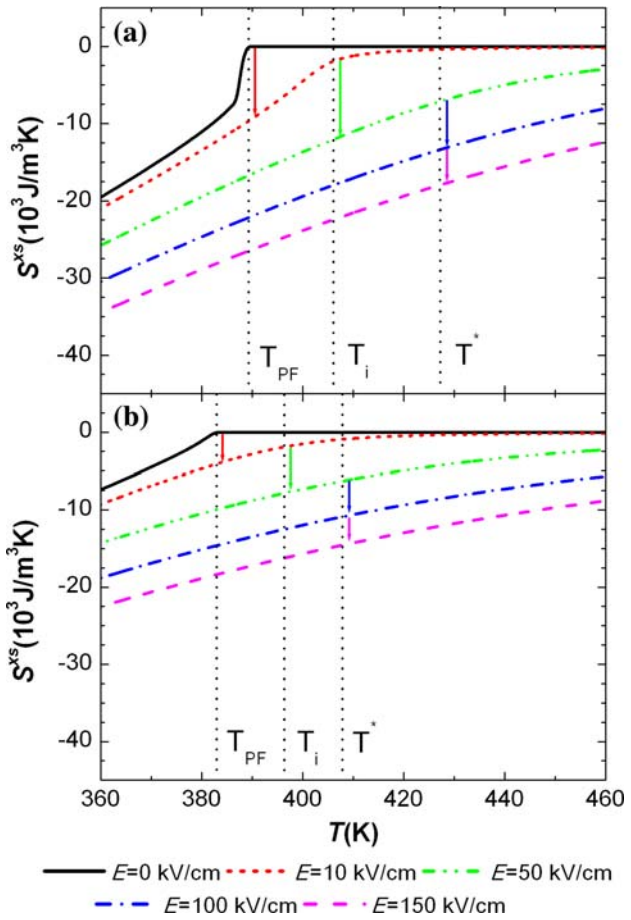

Fig. 4 Excess entropy as a function of temperature at different electric fields for **a** mechanically free (bulk) and **b** perfectly laterally clamped BTO. At $E = 0$ there is a discontinuity at the paraelectric–ferroelectric transition and as E increases this discontinuity disappears. The *vertical lines* mark the temperatures where the maximum change in entropy occurs for an electric field change ΔE having differing values of the bias field E_a and final field E_b as shown by the *arrows* (see text for details) (Color online)

$E_b > E_a$, the maximum change in entropy will always occur at the temperature of the first-order zero-field FE phase transition $T = T_{PF}$. This occurs because the majority contribution to the entropy change at this temperature is not due to the EC effect, but instead arises from the discontinuous change in entropy ΔS^{XS} at the first-order transition, $\Delta S^{XS} = L/T_{PF}$, where L is the latent heat.

Alternatively, if the field increase is made to take place starting from a much higher field that is sufficient to cause the discontinuities at T_{PF} to disappear as discussed above (e.g., $E^* = 50$ kV/cm), the maximum entropy change will always occur at some higher temperature $T = T^*$. On the other hand, when the field is increased from an intermediate nonzero value, e.g., $E_a = 10$ kV/cm $< E^*$, the maximum entropy change will occur at some different but intermediate temperature $T_{PF} < T_i < T^*$. Consequently, it is clear that when the electric field is changed between two values E_a and E_b, both the magnitude of the EC effect and temperature at which it is maximized depend not only on the extent of the field change $\Delta E = E_b - E_a$ but also on the value of the initial field E_a. It follows that under mechanically clamped conditions, where the zero-field PE–FE transition is of second-order, E^* may adopt a smaller value compared with that for the mechanically free crystal.

Under experimental conditions, E_a is a bias field and the field difference ΔE is the deviation above this bias. It is an important parameter to be specified, and it depends not only on the mechanical boundary conditions but also on the nature of the phase change in the bulk crystal. This is the case that is evident from Fig. 5, where the field dependence of the excess entropy as function of temperature for PTO is plotted. Again, the qualitative results are the same as those for BTO, but owing to the stronger first-order phase change in PTO, they differ quantitatively. For PTO, it is clear that even under clamped conditions, the shapes of the entropy-temperature curves will continue to evolve with electric field, even if a bias field as large as 150 kV/cm were to be

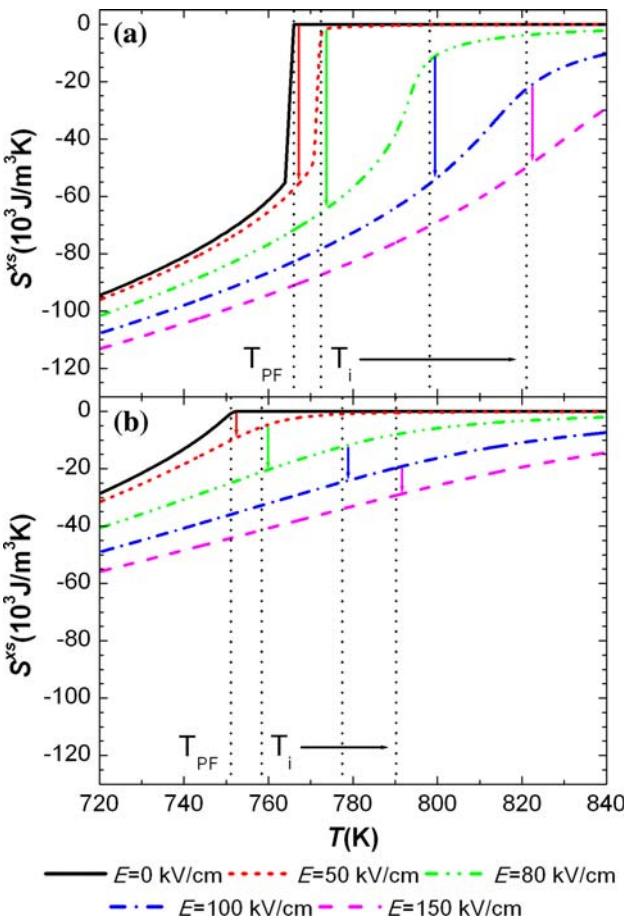

Fig. 5 Excess entropy as a function of temperature at different electric fields for **a** mechanically free (bulk) and **b** perfectly laterally clamped PTO (Color online)

applied. As a result, the maximum in the EC effect observed for differing values of ΔE above this bias will be displaced to lines of progressively higher temperatures. Because of the stronger first-order phase change in PTO as compared with BTO, a much larger bias field is required to minimize the dependence of the EC effect on temperature. For comparison, the entropy–temperature curves for STO are shown in Fig. 6. For STO, the primary effect of an electric field is to produce a small displacement of these curves toward the origin, relative to the zero-field temperature T_{st} of the second-order ferroelastic transition, as a consequence of the change in the excess specific heat due to the temperature and field dependencies of the structural order parameter.

The adiabatic temperature changes corresponding to the EC and electrothermal effects occurring near the ferroelectric and ferroelastic phase transitions in BTO, PTO, and STO can be computed using Eq. 30. These are compared in Fig. 7 as functions of temperature and electric field change, ΔE. In all cases the field change ΔE is taken relative to a bias field of $E_a = 50$ kV/cm. The results for BTO, PTO, and STO under mechanically free conditions are compared in Fig. 7a, c, and e, and the corresponding results obtained under perfect lateral clamping are compared in Fig. 7b, d, and e, respectively. It is seen that for this choice of bias field the adiabatic temperature change occurring near the first-order phase change in BTO under mechanically free conditions is modest, with a maximum value of $\Delta T \sim 1.6$ K. For the stronger first-order change in PTO the maximum EC effect is much larger, $\Delta T \sim 9$ K, but the effect is far more sensitive to temperature than it is for BTO under the same conditions. In STO, there is no true EC effect, and the temperature change arising from the change in the excess specific heat near the second-order structural phase transition is very small, $\Delta T < 0.5$ K. For BTO and PTO mechanical clamping transforms the first-order transitions into second-order ones, and so at the same bias field, both the magnitude and the temperature dependence of the EC ΔT are reduced. For the stronger first-order phase change in PTO, it is evident based on the results described above that an increase in the bias field to a value $E_a > 150$ kV/cm would further reduce the temperature sensitivity. As may be expected, for STO, mechanical clamping has no appreciable effect on the electrothermal temperature change.

The data shown in Fig. 7 also provides a qualitative indication concerning how the EC response of solid solutions comprising BTO, PTO, and/or STO as end member compounds may be expected to change with composition under the specific boundary conditions investigated. In the pseudo-binary phase diagrams of these systems, both the Curie temperature and the first-order character of the ferroelectric phase transition can be continuously varied with composition. For example, in the pseudo-binary solid solution $BaTiO_3$–$SrTiO_3$ (BST) the Curie temperature can be decreased from that of BTO ($\sim$383 K) over a temperature range extending down to about 150 K. In this instance, the composition change plays a role analogous to effect of hydrostatic pressure, and the order of the ferroelectric transition continually decreases toward a tricritical point as the strontium concentration is increased. The nature of the phase change, for a given composition (and hence Curie point), may, however, also be modified by compressive or tensile misfit strains arising from thermal stresses or lattice mismatch with the substrate. In choosing a ferroelectric material with a Curie temperature appropriate for use in a given temperature range, the electrical and mechanical boundary conditions can be adjusted, in conjunction with composition, in order to alter the nature of the phase change.

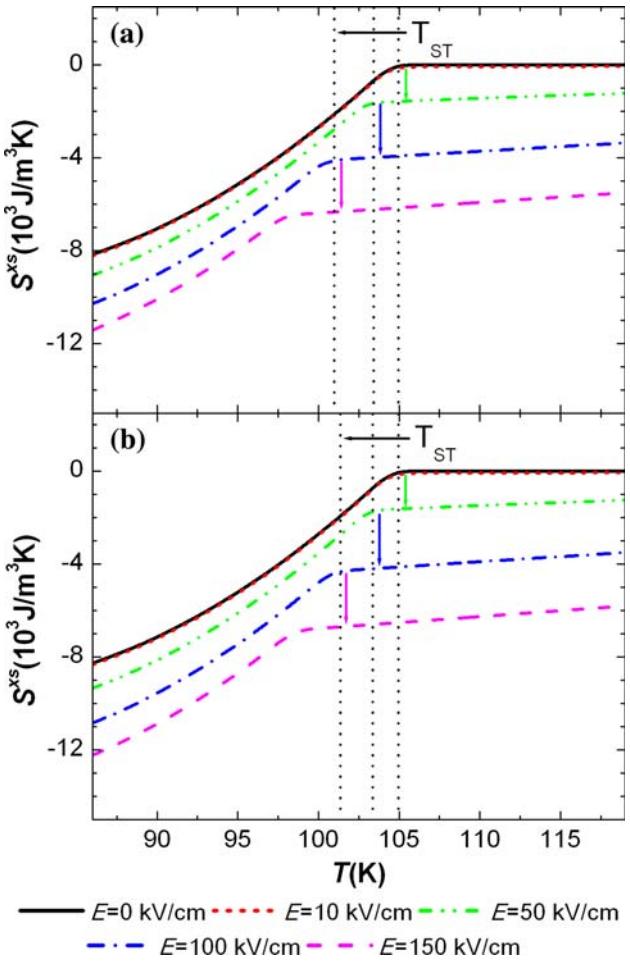

Fig. 6 Excess entropy as a function of temperature at different electric fields for **a** mechanically free (bulk) and **b** perfectly laterally clamped STO near the structural phase transformation temperature (Color online)

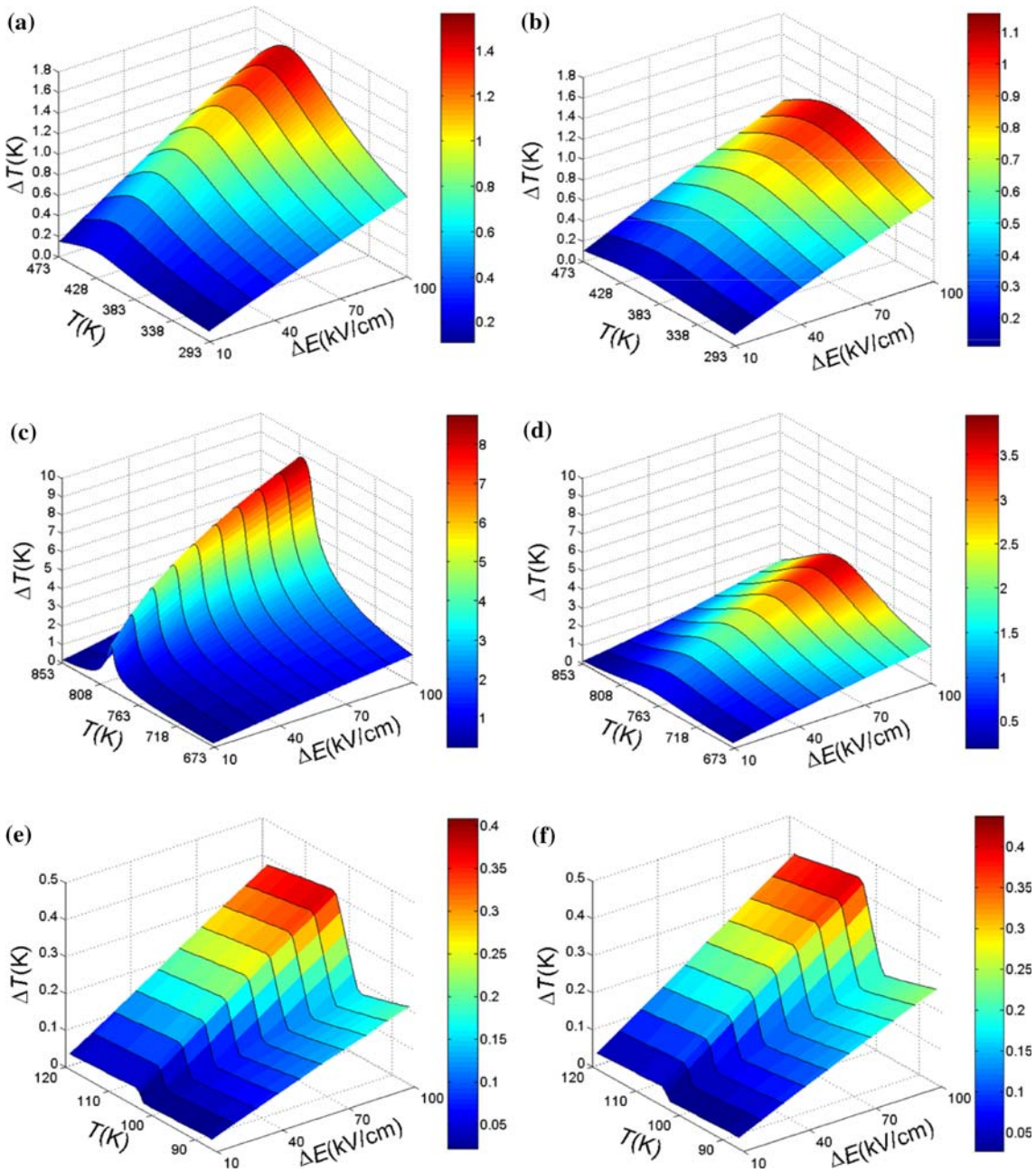

Fig. 7 Three-dimensional plots of the adiabatic temperature change ΔT as functions of T and ΔE ($E_a = 50$ kV/cm) for monodomain uniaxial **a**, **c**, and **e** unclamped stress-free (bulk) BTO, PTO, and STO, respectively, and **b**, **d**, and **f** BTO, PTO, and STO thin films with $u_m = 0$, respectively (Color online)

Conclusions

From the analysis presented above, several conclusions can be drawn that are relevant in investigations of the EC properties of ferroelectric materials. First, for ferroelectrics such as BTO and PTO displaying weak first-order transitions close to second-order, the use of a bias field is most likely essential in obtaining reproducible results under experimental conditions. For a given set of mechanical boundary constraints, the magnitude of this bias field would be comparable to the electrical critical point. The application of a bias field of greater magnitude reduces the sensitivity of the EC effect to temperature, but of course, also reduces the magnitude of the effect itself. Materials with stronger first-order phase transitions will naturally require a higher bias field. Under conditions of perfect

mechanical clamping, the weak first-order phase change as displayed by BTO and PTO will become of second-order, and in this instance the electrical critical point is coincident with the Curie temperature. As a consequence, a lower bias field will be sufficient to produce a comparable set of measurement conditions. Compressive or tensile misfit strains arising from thermal stresses or lattice mismatch with the substrate may also alter the nature of the phase change, and so the electric bias field may be shifted to higher or lower values. Alternatively, in solid solution ferroelectric systems, both the Curie temperature and the first-order character of the ferroelectric phase transition also change continuously with composition. The cooperative effect on the phase transition of mechanical boundary constraints, electric drive conditions and composition, is an important consideration in interpreting experimental observations of electrothermal phenomena in ferroelectric thin film materials selected to have Curie points located in a desired temperature range.

Acknowledgements The work at UConn was supported through Grants administered by the U.S. Army Research Office (W911NF-05-1-0528 and W911NF-08-C-0124) and the Office of Naval Research (N00014-09-1-0354). Two of the authors (S. P. Alpay and G. A. Rossetti) would like to thank Professor J. F. Scott for illuminating exchanges in connection with the work reported.

References

1. Childress JD (1962) J Appl Phys 33:1793
2. Fatuzzo E, Kiess H, Nitsche R (1966) J Appl Phys 37:510
3. Thacher PD (1968) J Appl Phys 39:1996
4. Mischenko AS, Zhang Q, Scott JF, Whatmore RW, Mathur ND (2006) Science 311:1270
5. Mischenko AS, Zhang Q, Whatmore RW, Scott JF, Mathur ND (2006) Appl Phys Lett 89:242912
6. Akcay G, Alpay SP, Mantese JV, Rossetti GA Jr (2007) Appl Phys Lett 90:252909
7. Akcay G, Alpay SP, Rossetti GA Jr, Scott JF (2008) J Appl Phys 103:024104
8. Dunne LJ, Valant M, Manos G, Axelsson AK, Alford N (2008) Appl Phys Lett 93:122906
9. Prosandeev S, Ponomareva I, Bellaiche L (2008) Phys Rev B 78:052103
10. Qiu JH, Jiang Q (2008) Phys Lett A 372:7191
11. Qiu JH, Jiang Q (2008) J Appl Phys 103:084105
12. Qiu JH, Jiang Q (2008) J Appl Phys 103:034119
13. Khodayari A, Pruvost S, Sebald G, Guyomar D, Mohammadi S (2009) IEEE Trans Ultrason Ferroelectr Freq Control 56:693
14. Neese B, Lu SG, Chu BJ, Zhang QM (2009) Appl Phys Lett 94:042910
15. Qiu JH, Jiang Q (2009) J Appl Phys 105:034110
16. Neese B, Chu B, Lu S, Wang Y, Furman E, Zhang QM (2008) Science 321:821
17. Devonshire AF (1949) Philos Mag 40:1040
18. Devonshire AF (1951) Philos Mag 42:1065
19. Uwe H, Sakudo T (1976) Phys Rev B 13:217
20. Fuchs D, Schneider CW, Schneider R, Rietschel H (1999) J Appl Phys 85:7362
21. Haeni JH, Irvin P, Chang W, Uecker R, Reiche P, Li YL, Choudhury S, Tian W, Hawley ME, Craigo B, Tagantsev AK, Pan XQ, Streiffer SK, Chen LQ, Kirchoefer SW, Levy J, Schlom DG (2004) Nature 430:758
22. Alpay SP, Misirlioglu IB, Sharma A, Ban Z-G (2004) J Appl Phys 95:8118
23. Pertsev NA, Zembilgotov AG, Tagantsev AK (1998) Phys Rev Lett 80:1988
24. Qiu QY, Nagarajan V, Alpay SP (2008) Phys Rev B 78:064117
25. Pertsev NA, Tagantsev AK, Setter N (2000) Phys Rev B 61:825